Journal of Applied Physics

Charge transport in cross-linked PEDOT:PSS near metal–insulator transition

Cite as: J. Appl. Phys. **131**, 155101 (2022); https://doi.org/10.1063/5.0085374
Submitted: 16 January 2022 • Accepted: 29 March 2022 • Published Online: 18 April 2022

Arya Mohan, A. G. Anil, P. C. Ramamurthy, et al.

Journal of Applied Physics ARTICLE scitation.org/journal/jap

Charge transport in cross-linked PEDOT:PSS near metal–insulator transition

Cite as: J. Appl. Phys. **131**, 155101 (2022); doi: 10.1063/5.0085374
Submitted: 16 January 2022 · Accepted: 29 March 2022 ·
Published Online: 18 April 2022

Arya Mohan,[1,a)] A. G. Anil,[2] P. C. Ramamurthy,[2] and Reghu Menon[1]

AFFILIATIONS

[1]Department of Physics, Indian Institute of Science, Bangalore 560012, India
[2]Department of Materials Engineering, Indian Institute of Science, Bangalore 560012, India

[a)]**Author to whom correspondence should be addressed:** aryamohan@iisc.ac.in

ABSTRACT

The charge transport in poly(3,4-ethylenedioxythiophene):poly(styrenesulfonate) cross-linked with divinyl sulfone (c-PEDOT:PSS) is compared with pristine PEDOT:PSS from conductivity, electric field, and frequency studies. In a cross-linked sample, the room temperature conductivity increased from 0.8 to 630 S/cm. The temperature dependence of conductivity, down to 4.2 K, is significantly weakened in a cross-linked sample. This cross-linking induced metal–insulator transition in PEDOT:PSS, as inferred from conductivity ratios ($\sigma_r = \sigma_{300K}/\sigma_{4.2K}$), shows the role of modified nanomorphology in charge transport. The values of σ_r for PEDOT:PSS and c-PEDOT:PSS are 6441 and 4.6, respectively. The temperature dependence of the electric-field effect on conductivity indicates that the nanoscale barriers for transport have been substantially reduced by cross-linking. Impedance spectroscopy studies suggest that the relaxation frequency in c-PEDOT:PSS is shifted to a higher frequency, and the real part decreases sharply at higher frequencies, indicating enhanced connectivity and weakened barriers between conductive PEDOT regions.

I. INTRODUCTION

It is well known that conductivity and charge transport properties of poly(3,4-ethylenedioxythiophene):poly(styrenesulfonate) (PEDOT:PSS) can be modified by altering the nanoscale morphology with the help of additives, such as dimethyl sulfoxide, ethylene glycol, sorbitol, etc.[1] Recent attempts have been made to chemically alter the nanostructures in PEDOT:PSS by cross-linking, and the preliminary studies show a large increase in conductivity. Since PEDOT:PSS is widely used in several commercial applications, it is important to find out how the modifications in structure and morphology affect charge transport properties. PEDOT:PSS is a water soluble polymer with nanoscale gel particles, it can easily swell and change the shapes in a solution, and the solid films tend to crack when exposed to humidity and other solvents. Cross-linking is one of the effective strategies to overcome some of these problems. Cross-linking of PEDOT:PSS can be done by physical cross-linking with non-conducting polymers,[2] chemical cross-linking,[3] and photo cross-linking with UV irradiation.[4] Organosilanes are widely used for chemical cross-linking of PEDOT:PSS, particularly (3-glycidoxypropyl) trimethoxysilane (GOPS).[5] These cross-linkers are mainly used to increase the stability of PEDOT:PSS for various applications; however, it does not enhance the conductivity to make it metallic-like.[6] Since this work focuses only on inducing the insulator to a metallic transition and making it more metallic, the best cross-linker is found to be DVS.[7] It is well known that PEDOT:PSS is widely used for transparent electrode applications in polymer and organic electronic and optoelectronic devices. Also, it is found to be a good hole transporter in organic devices.[8] In recent years, PEDOT:PSS is also being used in organic perovskite solar cell and other devices.[9,10] There have been earlier attempts to modify the work function by various chemical treatments to make it more compatible for specific applications, such as electrodes in devices.[11] In this context, DVS cross-linked PEDOT:PSS is found to be highly conducting and more stable. Mantione *et al.* have already used it in an organic electrochemical transistor for bioelectronic applications,[7] and Bora *et al.* have found it useful in EMI shielding.[12,13]

Previous charge transport studies in PEDOT:PSS have shown that a wide range of behavior from a metallic to an insulting side can be observed by varying the nanoscale morphology. The localized carriers in pristine PEDOT:PSS can be easily delocalized by extending the compact coil nanostructures, and this induces a

transition from an insulating to a metallic side of charge transport, as the temperature dependence of conductivity can be modified by several orders of magnitude.[14,15] However, this feature is not very well studied in chemically cross-linked PEDOT:PSS. In this work, the charge transport properties of DVS cross-linked PEDOT:PSS (c-PEDOT:PSS) are compared with a pristine one. In a cross-linked sample, the room temperature conductivity is increased to 630 from 0.8 S/cm, with the temperature dependence of conductivity down to 4.2 K substantially reduced by more than four orders of magnitude. This is further inferred from the reduced activation energy plots of W=d[ln(σ)]/d[ln(T)] vs T, in which the cross-linked sample shows a temperature independent W at low temperatures, as it is just on the metallic side of a metal–insulator transition,[16] whereas the slope of W in a pristine sample shows typical insulating behavior. The electric-field dependence of conductivity in a cross-linked sample shows strong field effects, with nonlinearity even at low fields, suggesting that cross-links have substantially weakened the nanoscale barriers for charge transport. This is further verified from impedance studies at 40 Hz-100 MHz in which the sharp decrease at 1 MHz for a pristine sample is significantly weakened by cross-linking and peak in imaginary part is rather small for the cross-linked sample.

II. EXPERIMENTAL DETAILS

The samples are prepared from PEDOT:PSS (Clevios PH1000) and divinyl sulfone (DVS) from Sigma-Aldrich. Cross linked PEDOT:PSS with DVS (c-PEDOT:PSS) is prepared from a solution of PEDOT:PSS with 5% by volume DVS and stirred for 20 min and then drop casted on a PET substrate. A free-standing film (15 μm) is formed after annealing at 50 $\pm$ 5°C. Similarly, pristine PEDOT:PSS films (25 μm) are made without the addition of DVS. Mantione *et al.*[7] have studied conductivity as a function of percentage of DVS. The maximum value of conductivity is observed around 5% of DVS. This maximum value at room temperature ensures that a highly conducting metallic state is possible even at 4.2 K. DVS is known to be highly reactive, so possibly used up in the cross-linking process, and any excess remaining is expected to be removed during annealing. Even if any traces of DVS are left in the sample, it is not going to affect the transport along the dense highly conducting network, so as to obtain 140 S/cm at 4.2 K. The advantages of using DVS are already discussed by Mantione *et al.*[7] In DVS cross-linked samples, the large increase in conductivity is highly reproducible with very consistent values, and it is stable for a long duration of time, even in the presence of other materials. This is very important in using it as a transparent electrode for device applications. Furthermore, in DVS cross-linked samples, the highly conducting metallic nature is retained even at 4.2 K (140 S/cm), which is quite rare in PEDOT:PSS samples. Since DVS cross-linked samples are both chemically and electronically more stable while compared to dimethyl sulfoxide or ethylene glycol processed samples, it is advisable for device applications. The same samples from the work of Bora *et al.*[12] is used in our experiments. The cross-sectional scanning electron microscopy (SEM) images show that c-PEDOT:PSS has coarser morphology when compared to the pristine PEDOT:PSS as shown in Fig. 1. The sulfonate group in PSS reacts with the vinyl group in DVS forming cross-links of a vinyl sulfone ethyl sulfonate structure between PEDOT:PSS chains. This feature is already verified from Fourier transform infrared (FTIR) spectra in earlier studies by other groups,[7] also in the work of Bora *et al.*[12] The FTIR spectrum of c-PEDOT:PSS films shows the presence of new absorption at 1313 cm^{-1} corresponding to OSO scissoring, which is a signature of cross-link formation between PEDOT:PSS and DVS as shown in Fig. 2. Absorption at 1055 cm^{-1} corresponds to S = O stretching of PSS.[12]

Four-probe DC conductivity and electric-field dependence are measured on freestanding films (0.1 cm × 0.5 cm). The contacts are made using conducting carbon paint, and values of contact resistances are below 100 Ω. Samples are mount to a custom-made low-temperature probe designed to work in standard liquid helium Dewar. DC conductivity measurements are done using a Keithley

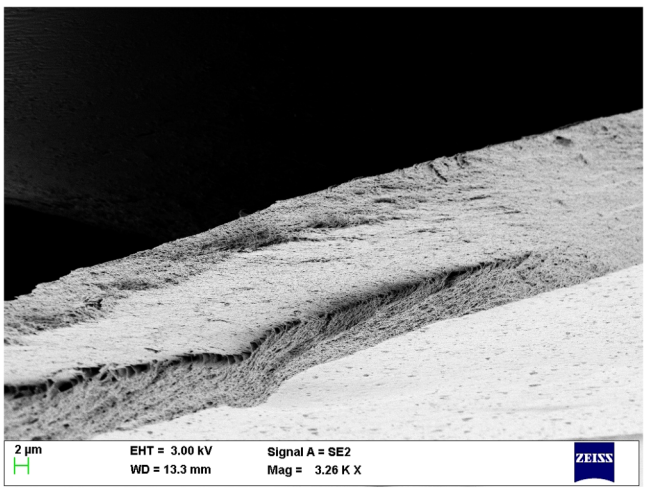

FIG. 1. Cross-sectional SEM image of c-PEDOT:PSS.

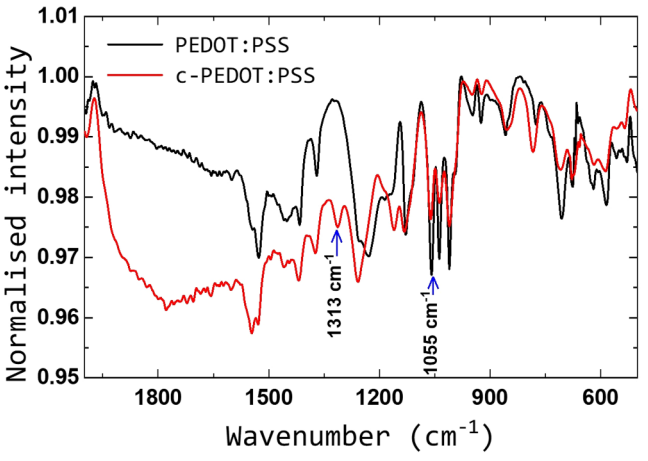

FIG. 2. FTIR spectra of PEDOT:PSS (black) and c-PEDOT:PSS (red).

sourcemeter (Model: 2400) and a Keithley multimeter (Model: 2000), down to 4.2 K. The temperature is measured and controlled by a Lakeshore controller (Model: 332) with a calibrated silicon diode sensor. Measurement and data acquisition are carried out with a LabVIEW program. Electric-field dependent conductivity studies are carried out by measuring currents under pulsed voltages from a Keithley sourcemeter (Model: 2400) at various stable temperatures down to 4.2 K. Both the DC conductivity (a very low field) and the electric-field dependent conductivity are carried out in the linear standard four-probe geometry all the way down to 4.2 K so that the comparison is quite straightforward. Room temperature impedance measurements are carried using Agilent impedance analyzer 4295A.

III. RESULTS AND DISCUSSION

A. Temperature dependent conductivity

It is well known that in complex materials, such as conducting polymers, the interplay of intrinsic one-dimensionality and disorder gives rise to a wide range of charge transport behavior. Furthermore, the complicated nanoscale morphology in PEDOT:PSS and its role in the conduction mechanism is yet to be fully understood. The transport measurements at $T > 80$ K are not adequate enough to unravel the localization phenomena and its role in metallic and insulating properties. In this work, the variation of transport in c-PEDOT:PSS is compared with the pristine sample. In this cross-linked sample, the altered structure and nanomorphology is shown to facilitate enhanced bulk transport.

The temperature dependence of conductivity of both types of PEDOT:PSS is carried out down to 4.2 K, as shown in Fig. 3. Upon cross-linking with DVS, the room temperature conductivity of PEDOT:PSS increases from 0.8 to 630 S/cm. The enhanced transport features in a cross-linked sample become more evident when the conductivity ratios $[\sigma_r = \sigma_{300\,\mathrm{K}}/\sigma_{4.2\,\mathrm{K}}]$ of these two samples are compared, and the σ_r values are 6441 and 4.6 for PEDOT:PSS and c-PEDOT:PSS, respectively. First, the conductivity values of pristine PEDOT:PSS are only 0.8 S/cm at room temperature; and second, it decreases significantly to 1.2×10^{-4} S/cm. This large variation usually occurs in insulating samples in which the disorder is very large, and the carriers require large activation energy to hop from one site to another site, whereas in a cross-linked sample, not only the room temperature conductivity is high (630 S/cm), but it retains its highly conducting state (140 S/cm) even at 4.2 K. This marked difference highlights that the electronic states are highly delocalized, with less important role played by disorder. These values show that pristine PEDOT:PSS is an insulator with dominant hopping type transport, and the cross-linked sample is near the metal–insulator transition. The increase in conductivity happens when the localized electronic states become delocalized due to the opening up and extension of the compact coil PEDOT:PSS chains as the cross-linker DVS forms a better network among nanoscale gel particles, to facilitate enhanced charge transport, as the barriers are significantly reduced.

The temperature dependence of conductivity data is analyzed in detail by reduced activation energy plots as shown in Fig. 4, and it is expressed as in Eq. (1),[16]

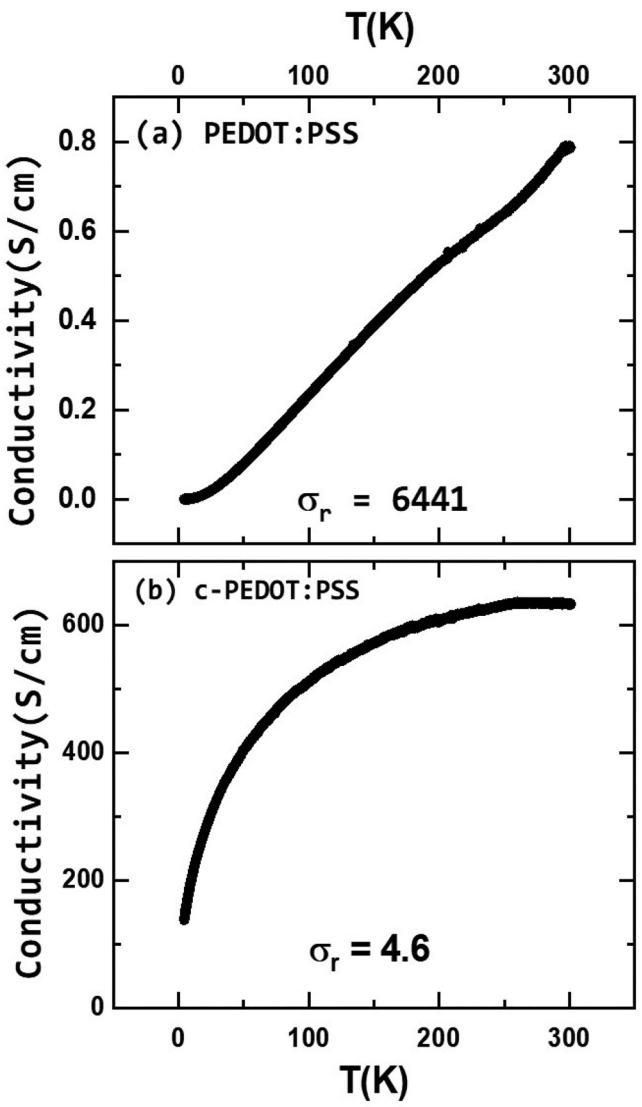

FIG. 3. Conductivity vs temperature: (a) pristine PEDOT:PSS and (b) c-PEDOT:PSS. Conductivity ratio ($[\sigma_r = \sigma_{300\,\mathrm{K}}/\sigma_{4.2\,\mathrm{K}}]$) is 6441 for PEDOT:PSS and 4.6 for c-PEDOT:PSS.

$$W = \frac{d[\ln(\sigma)]}{d[\ln(T)]}. \tag{1}$$

The slope of W vs T in pristine PEDOT:PSS increases with decreasing temperature, as expected in an insulator. However, W of c-PEDOT:PSS is nearly temperature independent, from 40 to 4.2 K, implying that the system is in the critical regime of a metal–insulator transition. Cross-linking of PEDOT:PSS with 5% of DVS modifies the nanoscale barriers for charge transport, and the increase in room temperature conductivity corroborates with the nearly

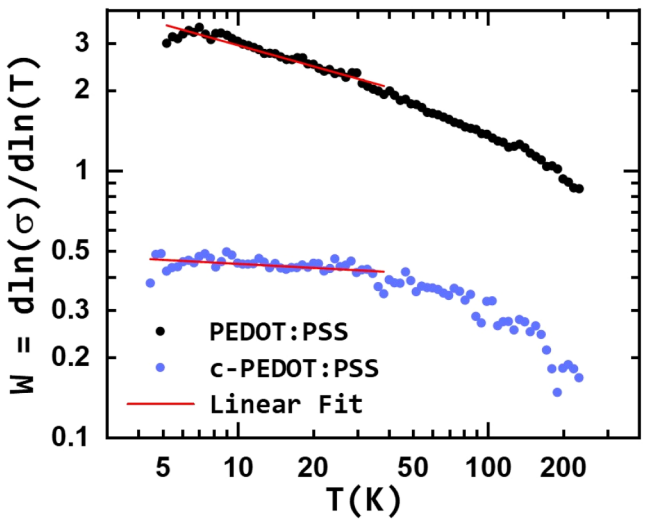

FIG. 4. Reduced activation energy W vs temperature in a log–log scale. PEDOT:PSS (black) in VRH and c-PEDOT:PSS(blue) is near a metal–insulator transition. The red line indicates a linear fit.

metallic-like weak temperature dependence of conductivity. The W plots in Fig. 4 give the exact functional temperature dependence of conductivity. The slope of W for PEDOT:PSS indicates exponential temperature dependence of conductivity [$\sigma \propto \exp(-(T_0/T)^{\gamma})$]. By taking the log of Eq. (1), $\log(W) = C - \gamma \log(T)$, the positive slope of a log(W) vs log(T) plot gives the exponent of temperature γ. A slope of 0.25 is obtained for PEDOT:PSS from a W plot, indicating 3D variable range hoping (VRH) transport, as given by

$$\sigma = \sigma_0 \exp -\left(\frac{T_0}{T}\right)^{+\frac{1}{4}}, \tag{2}$$

where T_0 is the characteristic temperature defined as $T_0 = \frac{\lambda}{k_B N(E_F) L_c^3}$, where λ is a constant value of 18.1, k_B is the Boltzmann constant, $N(E_F)$ is the density of states at the Fermi-level, and L_c is the localization length.[17,18] The conductivity of a system in a critical regime of a metal–insulator transition is given by

$$\sigma \approx (\hbar^2/e^2 p_F)(k_B T/E_F)^{1/\eta} \propto T^{\beta}, \tag{3}$$

where p_F is the Fermi momentum and e is the electronic charge.[19] η is predicted to be $1 < \eta < 3$ and $0.3 < \beta < 1$. The exponent β can be determined from $W = \beta$ in a critical regime, and its value is around 0.44. Therefore, the transport near a critical regime is very weakly activated, and it follows a power law dependence of temperature.

As deduced from a W plot, PEDOT:PSS is fitted to 3D VRH and c-PEDOT:PSS to power law dependence. Figure 5(a) shows conductivity of PEDOT:PSS in a natural log scale vs $T^{-1/4}$. A straight line fit to the data gives a slope value of 20.73, and the deduced value of T_0 is around 1.84×10^5 K. The value of T_0

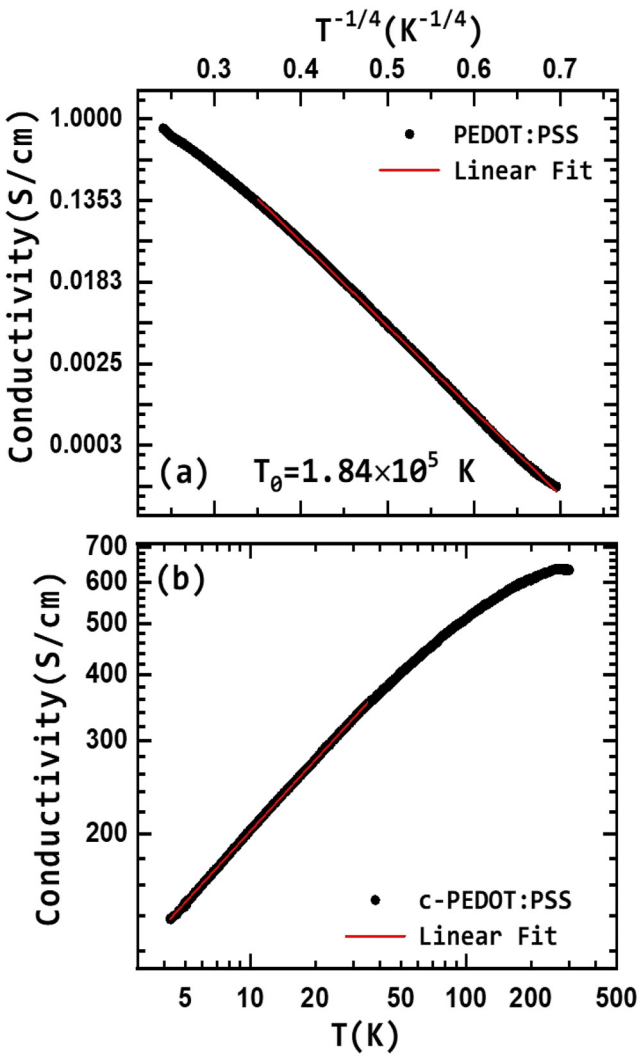

FIG. 5. (a) Conductivity vs $T^{-1/4}$ fit for PEDOT:PSS, showing 3D VRH. (b) Conductivity vs T in a log–log scale, showing power law near a metal–insulator transition.

obtained from $W(T) = 0.25(T_0/T)^{1/4}$ is in agreement with the value of T_0 obtained from the fit to Eq. (2). The large value of T_0 suggests that the localization is strong. From the approximate values of density of states from earlier studies[20] (10^{20} eV^{-1} cm^{-3}), a rough estimate of localization length is found to be 2.2 nm. However, for c-PEDOT:PSS in the critical regime, the Fermi energy E_F and mobility edge E_C come rather close. The low-temperature conductivity of a DVS cross-linked sample follows a power law, as in Fig. 5(b) with the value of exponent 0.44. This value of exponent at the critical regime of a metal–insulator transition denotes the role of disorder in the transition. For example, if the value is close to 0.3, it is more metallic with less disorder, and if it is near 1, then it is more toward the insulating side.[19]

B. Electric-field dependence

In Sec. III A, the DC transport was mainly focused in the low-field ohmic regime. It is known that in disordered systems, the barriers and localization can be altered by probing the electric-field dependence of transport at different temperatures. The current vs voltage plot of PEDOT:PSS shows a symmetrically linear behavior up to 4 V, in both directions of applied voltage, at various temperatures from 4.2 to 200 K, as shown in Fig. 6(a). At all temperatures, PEDOT:PSS remains in ohmic regime up to 4 V, indicating that there is no electric-field-induced nonlinearity, and the measured values of current are less than a few mA to avoid any sample heating, and at lower temperatures, measured values of current are typically in μA, as the sample conductivity goes down. Furthermore, sample and sensor are in very close proximity so that any temperature fluctuation can be immediately monitored. Since the conductivity of PEDOT:PSS varies by several orders of magnitude as a function of temperature, the current values vary from μA to mA for the same applied voltage. The current vs voltage of c-PEDOT:PSS is shown at different temperatures in Fig. 6(b) up to

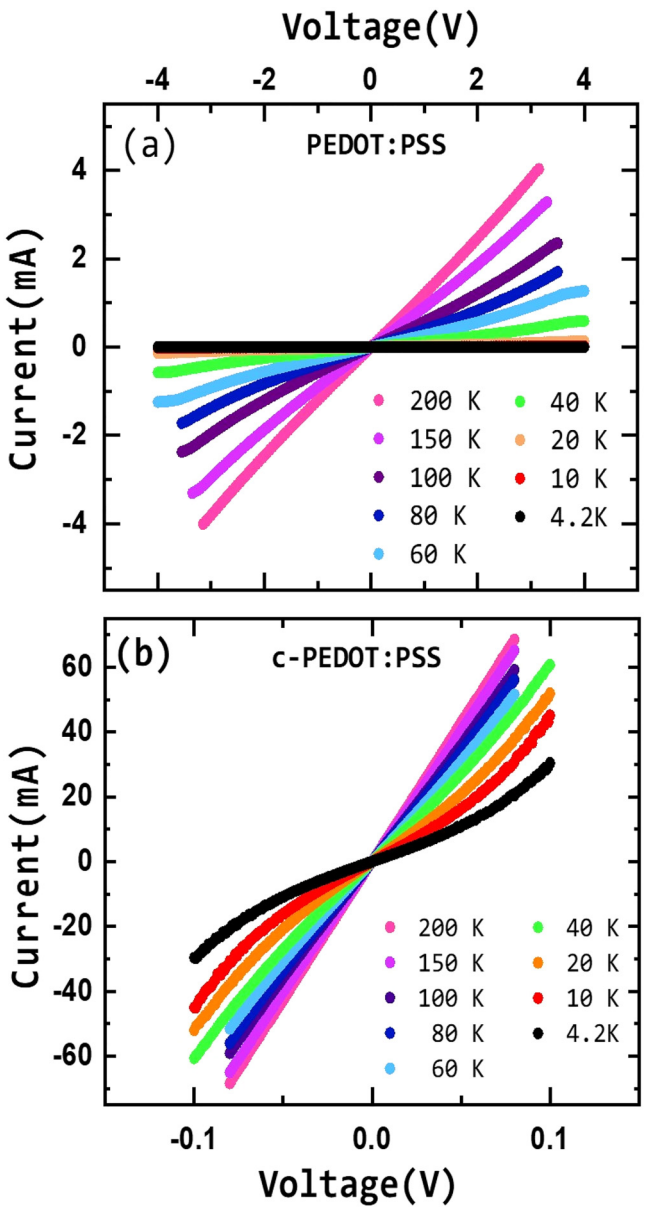

FIG. 6. Current vs voltage: (a) PEDOT:PSS and (b) c-PEDOT:PSS, showing nonlinear behavior below 40 K.

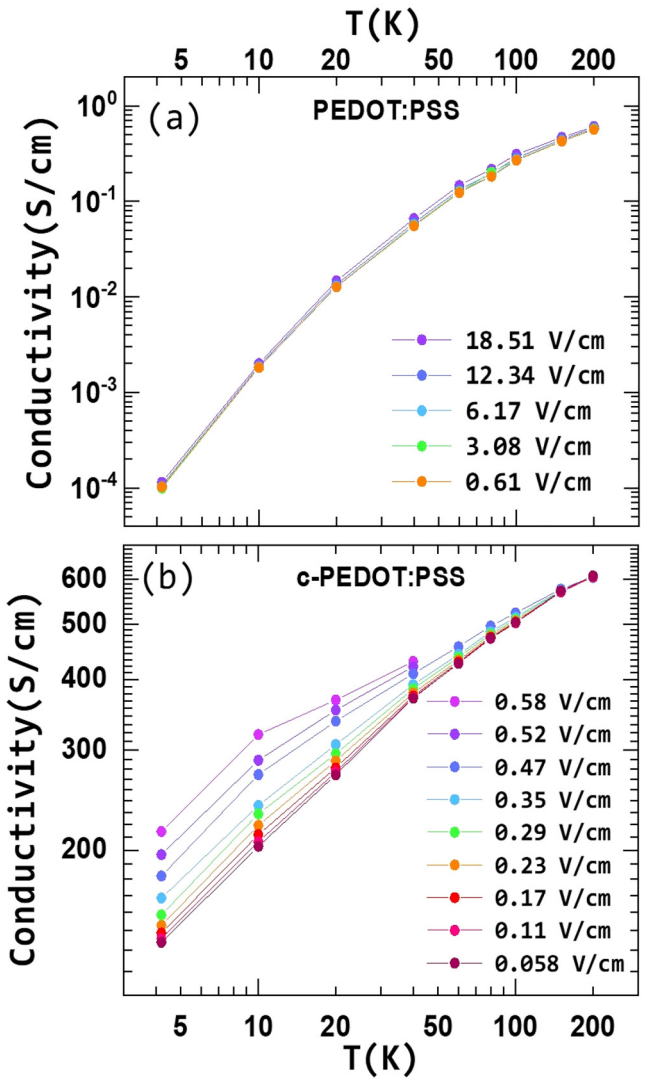

FIG. 7. Conductivity vs temperature at various electric fields: (a) PEDOT:PSS and (b) c-PEDOT:PSS.

0.1 V. From 4.2 to 40 K, current increases nonlinearly with voltage, and above 40 K, it becomes more linear. This shows that the electric field is modifying the barriers for low-temperature transport in c-PEDOT:PSS, as the nanoscale morphology is altered by cross-linking. This is possible even at 0.1 V, indicating that the shallow barriers are further lowered in the presence of such low fields. Hence, this observation is consistent with the weak temperature dependence of conductivity in this sample.

The temperature dependent conductivity of PEDOT:PSS and c-PEDOT:PSS at different electric fields is shown in Figs. 7(a) and 7(b), respectively. The conductivity data of PEDOT:PSS at different electric fields from 0.61 to 18.51 V/cm all tend to merge on top of each other, suggesting hardly any electric-field dependence in the applied range, whereas the conductivity of c-PEDOT:PSS shows a significant change in conductivity as the electric field is varied. Especially at low temperatures, conductivity increases with an increase in electric field, from 0.058 to 0.58 V/cm. This effect becomes weaker at higher temperatures as the curves tend to merge. At higher temperatures, the electric-field effect becomes less significant. To understand the electric field dependence more clearly, conductivity is plotted as a function of electric field at different temperatures for PEDOT:PSS and c-PEDOT:PSS in Fig. 8. The conductivity of PEDOT:PSS hardly varies for fields upto 25 V/cm at all temperatures. This nearly electric-field independence on conductivity in PEDOT:PSS suggests that barriers are quite large, and the applied field is not enough to provide the activation energy required to overcome the barriers. However, conductivity of c-PEDOT:PSS increases with the electric field even at such low fields as 0.58 V/cm, at low temperatures. The conductivity is constant up to some field and then it increases at higher fields. This onset in an increase in conductivity moves to higher fields, as the temperature increases. This indicates that as the carriers get thermally activated at higher temperatures, its field effect becomes weaker, and it becomes nearly field independent.

This increase in conductivity in c-PEDOT:PSS as a function of electric field at temperatures below 40 K are further analyzed as shown in Fig. 9. A linear fit at higher electric fields for the data in the temperature range of 4.2–40 K has a slope of 0.5–0.2. As the carriers get activated by electric field to overcome the barriers, the conductivity increases, especially at $T < 40$ K. Even as the applied field has to be limited below 0.6 V/cm to avoid any sample heating at low temperatures, this large increase in conductivity is attributed to the gain in energy for transport from the field. Since the conductivity of c-PEDOT:PSS is nearly 140 S/cm at 4.2 K, which is quite large, the barriers are already shallow, and even low field can provide energy to overcome it.

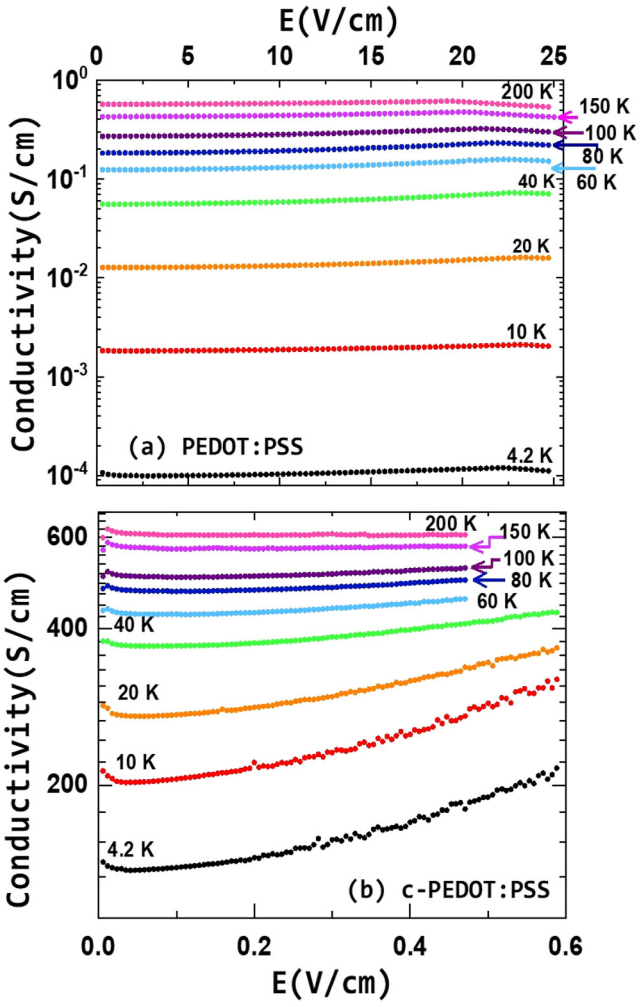

FIG. 8. Conductivity vs electric field at various temperatures: (a) PEDOT:PSS and (b) c-PEDOT:PSS.

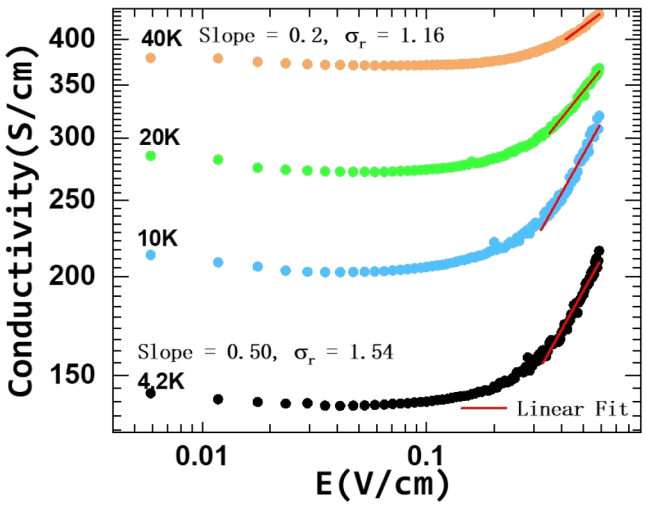

FIG. 9. Conductivity vs electric field of c-PEDOT:PSS in a log–log scale (4.2–40 K). Conductivity ratio ($\sigma_r = \sigma_{0.58\,V/cm}/\sigma_{0.1\,V/cm}$) is 1.54 at 4.2 K and 1.16 at 40 K.

C. Frequency dependence

The frequency dependent impedance studies are expected to give some insight into the transport and associated relaxation processes in PEDOT:PSS and c-PEDOT:PSS. The frequency dependence of real and imaginary parts of impedance for PEDOT:PSS and c-PEDOT:PSS, respectively, is shown in Figs. 10(a) and 10(b). The impedance value of PEDOT:PSS is higher than c-PEDOT:PSS, and the frequency response is less significant in c-PEDOT:PSS. The real part of impedance of PEDOT:PSS decreases rapidly around 1 MHz, showing a higher time constant for the relaxation of charge carriers in an alternating electric field, while the real part of impedance of c-PEDOT:PSS has a small reduction around 10 MHz implying a shorter relaxation time constant. The imaginary part of impedance of PEDOT:PSS has a large peak around 1.6 MHz, while c-PEDOT:PSS has a small peak at 14.8 MHz. The weak response in c-PEDOT:PSS at a higher frequency implies better connectivity among conductive PEDOT regions with significantly lowered barriers, as already implied from DC transport.

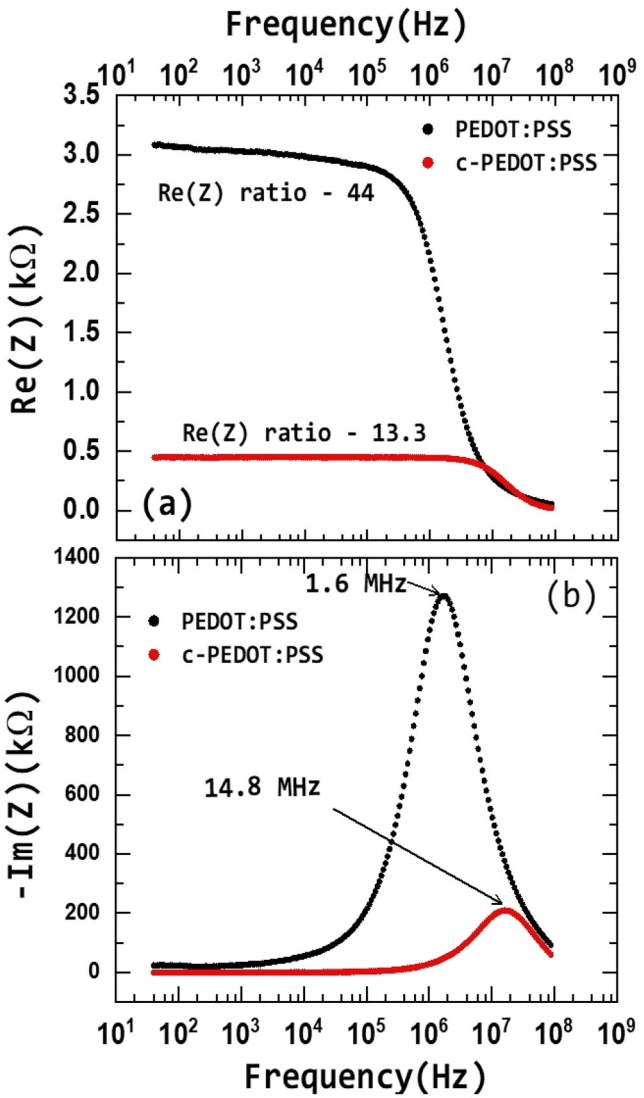

FIG. 10. Impedance vs frequency: (a) real part and (b) imaginary part.

IV. CONCLUSION

The conductivity of PEDOT:PSS increased from 0.8 to 630 S/cm by cross-linking with 5% of DVS. The conductivity ratios ($\sigma_r = \sigma_{300\,K}/\sigma_{4.2\,K}$) of PEDOT:PSS (6441) and c-PEDOT:PSS (4.6) show that latter is highly conducting and moved toward the metallic side of a metal–insulator transition. This becomes more evident from the reduced activation energy (W) plots showing that c-PEDOT:PSS is in the critical regime (constant W from $T < 40$ K), while the slope of W (T) shows PEDOT:PSS as an insulator. The low-temperature conductivity of c-PEDOT:PSS follows a power law, whereas PEDOT:PSS follows 3D VRH with a large value of T_0 (1.84×10^5 K). PEDOT:PSS hardly shows any field dependence of conductivity (up to 25 V/cm) at all temperatures, implying that the nanoscale barriers are large, whereas in c-PEDOT:PSS, a strong electric-field dependence is observed even at fields as low as 0.58 V/cm, indicating significantly weakened barriers. The I–V of PEDOT:PSS is linear and ohmic, whereas in c-PEDOT:PSS, it becomes nonlinear at low temperatures. These results show that cross-linking has improved the nanoscale morphology in PEDOT:PSS with reduced barriers for charge transport. These are further corroborated from impedance studies at 40 Hz–100 MHz. The real part of impedance shows a sharp decrease at 1 MHz for PEDOT:PSS, and only a minor decrease is observed in c-PEDOT:PSS at 10 MHz. Similarly, the imaginary part of impedance shows a sharp peak at 1.6 MHz for PEDOT:PSS and a rather small one at 14.8 MHz for c-PEDOT:PSS. These indicate that the relaxation time constant is lowered by improving the connectivity in c-PEDOT:PSS.

AUTHOR DECLARATIONS

Conflict of Interest

The authors have no conflicts to disclose.

DATA AVAILABILITY

The data that support the findings of this study are available from the corresponding author upon reasonable request.

REFERENCES

[1]P. Stadler, D. Farka, H. Coskun, E. D. Głowacki, C. Yumusak, L. M. Uiberlacker, S. Hild, L. N. Leonat, M. C. Scharber, P. Klapetek, R. Menon, and N. S. Sariciftci, J. Mater. Chem. C **4**, 6982 (2016).
[2]S. Ghosh and O. Ingangs, Synth. Met. **101**, 413 (1999).
[3]T.-M. Huang, S. Batra, J. Hub, T. Miyoshi, and M. Cakmak, Polymer **54**, 6455 (2013).
[4]X. YingJie, Q. MinFang, W. GuiWei, Z. GengMin, G. DengZhu, and W. U. JinLei, Sci. China Technol. Sci. **57**, 44 (2014).
[5]R. Colucci, G. C. Faria, L. F. Santos, and G. Gozzi, J. Mater. Sci.: Mater. Electron. **30**, 16864 (2019).
[6]A. Hakansson, S. Han, S. Wang, J. Lu, S. Braun, M. Fahlman, M. Berggren, X. Crispin, and S. Fabiano, J. Polym. Sci., Part B: Polym. Phys. **15**, 814–820 (2017).

[7]D. Mantione, I. del Agua, W. Schaafsma, M. ElMahmoudy, I. Uguz, A. Sanchez-Sanchez, H. Sardon, B. Castro, G. G. Malliaras, and D. Mecerreyes, ACS Appl. Mater. Interfaces **9**, 18254–18262 (2017).
[8]Q. B. Ke, J.-R. Wu, C.-C. Lin, and S. H. Chang, Polymers **14**, 823 (2022).
[9]C. Duan, Z. Liu, L. Yuan, H. Zhu, H. Luo, and K. Yan, Adv. Opt. Mater. **8**, 2000216 (2020).
[10]K. M. Reza, A. Gurung, B. Bahrami, S. Mabrouk, H. Elbohy, R. Pathak, K. Chen, A. H. Chowdhury, M. T. Rahman, S. Letourneau, H.-C. Yang, G. Saianand, J. W. Elam, S. B. Darling, and Q. Qiao, J. Energy Chem. **44**, 41 (2020).
[11]D.-J. Yun, J. J.-H. Kim, H. Ra, J.-M. Kim, B. S. Choi, J. Jang, M. Seol, and Y. J. Jeong, Appl. Surf. Sci. **553**, 149584 (2021).
[12]P. J. Bora, A. G. Anil, K. J. Vinoy, and P. C. Ramamurthy, Adv. Mater. Interfaces **6**, 1901353 (2019).
[13]P. J. Bora, A. G. Anil, P. C. Ramamurthy, and D. Q. Tan, Mater. Adv. **1**, 177 (2020).
[14]D. Bagchi and R. Menon, Chem. Phys. Lett. **425**, 114 (2006).
[15]P. K. Choudhury, D. Bagchi, C. S. S. Sangeeth, and R. Menon, J. Mater. Chem. **21**, 1607 (2011).
[16]A. G. Zabrodskii and K. N. Zinov'eva, Zh. Eksp. Teor. Fiz. **86**, 727 (1984) [Engl. trans. Sov. Phys. JETP **59**, 425 (1984)].
[17]N. Mott and E. Davis, *Electronic Processes in Non-Crystalline Materials* (Clarendon, Oxford, 1979).
[18]B. Shklovskii and A. Efros, *Electronic Properties of Doped Semiconductors* (Springer-Verlag, Berlin, 1984).
[19]A. I. Larkin and D. E. Khrnel'nitskil, Zh. Eksp. Teor. Fiz. **83**, 1140 (1982) [Engl. trans. Sov. Phys. JETP **56**, 645 (1982)].
[20]E. J. Bae, Y. H. Kang, K.-S. Jang, and S. Y. Cho, Sci. Rep. **6**, 18805 (2016).